Formation and fragmentation of negative metal clusters

K. Hansen,[1] J. U. Andersen,[1] J. S. Forster,[2] and P. Hvelplund[1]
[1]*Institute of Physics and Astronomy, Aarhus University, DK-8000 Aarhus C, Denmark*
[2]*Department of Engineering Physics, McMaster University, Hamilton, Ontario, Canada L8S 4L7*
(Received 13 December 1999; revised manuscript received 21 July 2000; published 3 January 2001)

We have measured the yield of metal cluster anions of Al, Co, Ni, and Cu produced in a sputter ion source, and also the distribution of negative fragment ions after collisions in gases of H_2 and Xe. For Al and Cu the fragment distributions show pronounced size effects that can be correlated with the stability of the species as reflected in the electron affinity. Modeling the collisional energy transfer, electron emission, and evaporation rates, we find that the fragment abundances are strongly influenced by thermal electron emission. The abundance spectra of the parent ions from the source show a similar correlation with the electron affinity, superimposed on a strong decrease with cluster size. For Co and Ni the negative-ion yields are much smaller than for Al and Cu, both from the source and after fragmentation, and this can be explained by even stronger neutralization by thermal electron emission.

DOI: 10.1103/PhysRevA.63.023201 PACS number(s): 36.20.Kd, 36.40.−c, 36.40.Qv, 39.10.+j

I. INTRODUCTION

Studies of cluster abundances give important information on cluster properties, as is evident from the discovery of the electronic shell structure in metal clusters by Knight *et al.* in sodium clusters [1] and by Katakuse *et al.* in coinage metal clusters [2]. In these experiments, the shell structure was reflected in strong anomalies in the cluster abundance as a function of the number of atoms in the cluster. The anomalies were observed as strongly enhanced abundances for the ''magic'' numbers $N=8$, 20, 40, etc. (9,21,41, . . . for the positively charged clusters) and appeared in the spectra without any manipulation of the cluster beam emitted from the source. Following the two seminal papers, a large effort has been devoted to the study of this phenomenon by a number of groups, using a variety of techniques such as threshold ionization, laser vaporization, collision-induced dissociation, abundance studies, etc., and a wide range of sources producing clusters of most metallic elements. The majority of these cluster sources are based on the formation of clusters through aggregation of monomers in a growth process (see [3] for a comprehensive review). Sputter sources are unique in producing clusters through the breakup of larger entities. This allows one to study not only properties of the clusters but also the sputtering process which is of considerable interest in itself. Both the source abundances and the size distributions arising from collisions are determined by mechanisms that are not understood in detail. This work attempts a comparison of the two using the electronic shell structure and the odd-even stability alternations as the link.

The cluster anions were produced in a sputter source of the Aarhus negative-ion source (ANIS) type [4] and were composed of four elemental metals: Al, Co, Ni, and Cu. Both the abundance spectra resulting from the formation process in the source and those resulting from fragmentation after collision with H_2 or Xe were recorded. The abundances are correlated with literature values of electron affinities determined by optical spectroscopy.

II. EXPERIMENT AND RESULTS

The experimental setup has been described in detail elsewhere [5] and only a brief overview is given here. It consists of three sections: (1) the production region consisting of an ion source, an accelerator, and a high-resolution magnet, (2) the interaction region, a differentially pumped gas cell, and (3) the detection region, a hemispherical electrostatic analyzer equipped with a ceratron detector connected to a computer.

Negative clusters produced by Cs^+ sputtering at 2 kV of Al, Co, Ni, or Cu cathode material were accelerated to 50 keV, magnetically mass separated, and passed through the gas cell. When the cell was pressurized to approximately 1 mbar of H_2 or Xe, cluster-gas collisions produced a measurable number of fragments. The fragments exited the cell and drifted for 1.4 m in a field-free region before entering the electrostatic analyzer. At the high acceleration energies used, the velocity of the fragments is virtually identical to that of the parent cluster ion, and the electrostatic analyzer therefore measures the mass of the fragment. Only the negative fragments were detected in the experiments. Positive fragments were also measured but their abundance was in all cases smaller by orders of magnitude than that of the negative ions. The neutral channel could not be detected by electrostatic deflection, but its presence can be inferred from the difference between the loss of the parent signal and the total yield of charged fragments. For Al and Cu clusters it was found that the neutral channel and the negative fragment channel were of similar magnitude. The fraction of charged fragments increased with cluster size for Al but was fairly constant for Cu. In both cases collisions with Xe neutralized about twice as effectively as collisions with H_2. In contrast to Al and Cu, the neutral channel was dominant for both Co and Ni.

A typical fragmentation spectrum, for a beam of Cu_9^- on H_2, is shown in Fig. 1. Since the energy interval accepted by the analyzer is proportional to the energy, each fragment peak area was corrected through division by its energy. The fraction of the incident beam that resulted in a particular

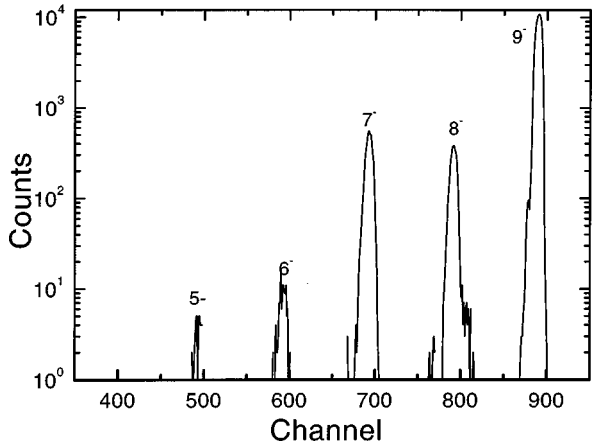

FIG. 1. Spectrum of Cu_N^- fragments from collisions of Cu_9^- clusters with H_2 molecules.

cluster mass was then obtained as the corrected peak area divided by the counts corresponding to an unattenuated beam. Results for Al_N^- and Cu_N^- clusters are shown in Figs. 2 and 3, respectively.

To determine the source abundance spectrum, the gas was pumped out of the cell, the analyzer set to the incident beam energy, and the magnetic field in the mass separator was scanned. Because of the rapid change of fragment intensity with cluster size it was necessary to divide the scan into several runs, with overlapping masses for normalization, using varying beam aperture sizes. Figure 4 shows source abundances for Al_N^- and Cu_N^- clusters, where the intensity can be seen to vary by up to seven orders of magnitude over the cluster sizes studied.

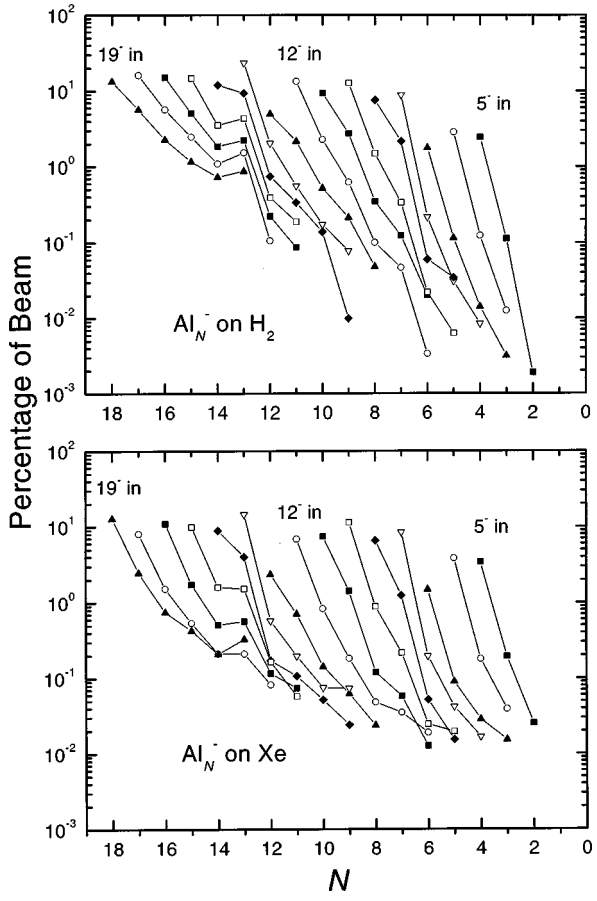

FIG. 2. Distribution of negative fragments for Al_N^- beams colliding with H_2 and Xe.

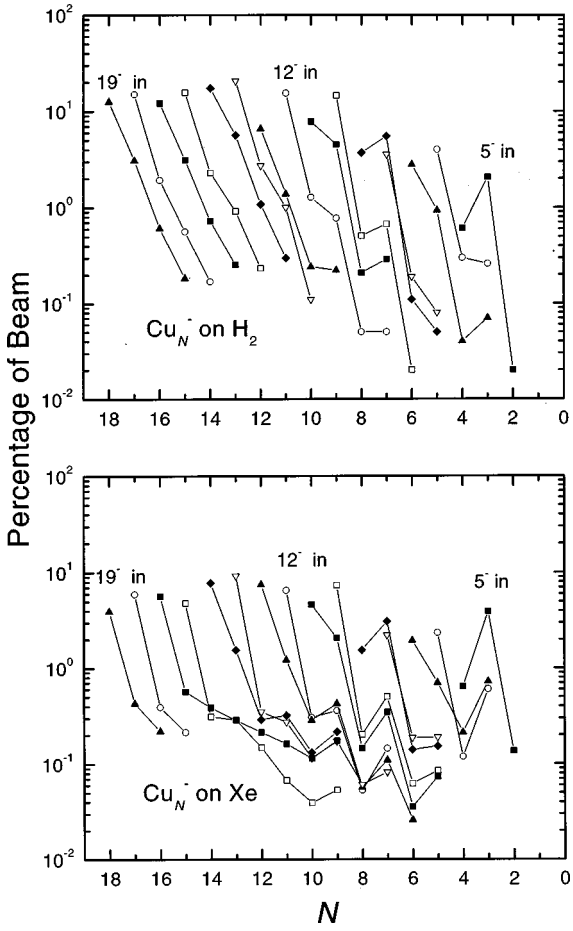

FIG. 3. Distribution of negative fragments for Cu_N^- beams colliding with H_2 and Xe.

Only Al and Cu gave appreciable count rates for cluster sizes above 7–8, but even below, the overall production of Co and Ni anions was markedly smaller than for Al and Cu. The small yield of Co and Ni anionic fragments can be ascribed to the efficient thermionic emission decay for these elements [12]. The strong tendency to emit electrons in collisions corroborates this suggestion.

III. DATA ANALYSIS

Figure 4 shows that for both Al and Cu the source intensity decreases rapidly with increasing size. Superimposed on this general trend there are marked short-range variations in the abundances. In particular, the odd-even alternations are pronounced for Cu. In order to display these structures more clearly, the following procedure was used: The abundances were fitted with a smooth function (also shown in Fig. 4), a modified exponential $\ln(I_N)=c_1+c_2N^{-n}+c_3N$, with $c_2=-6$, $n=0.7$, and $c_3=1.6$ (for Al) and $\ln(I_N)=c_1+c_2N^{-n}$,

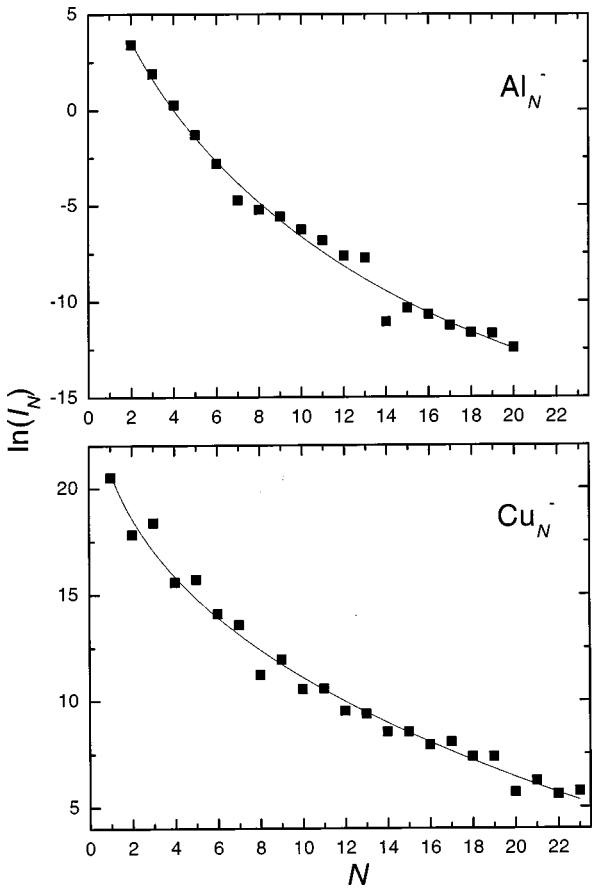

FIG. 4. Magnet scans for Al_N^- and Cu_N^- from a sputter source. The curves are smooth fits, with parameters given in the text.

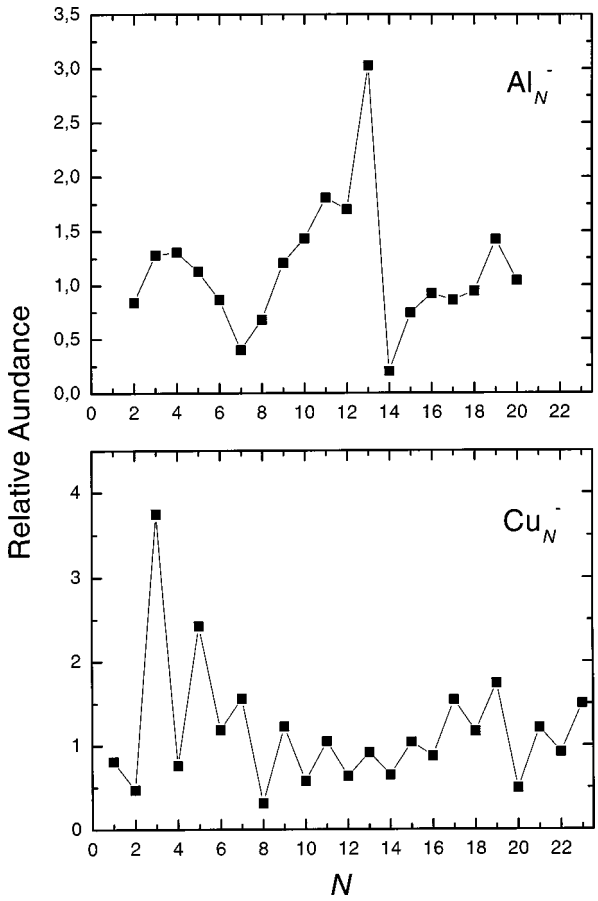

FIG. 5. Magnet scans for Al_N^- and Cu_N^- after division by a smooth function of *N*.

with $c_2=-8$ and $n=0.34$ (for Cu). The smooth function was then divided out, leaving abundances oscillating about unity as shown in Fig. 5. The smooth curve is determined mainly by the physics of cluster formation at or close to the surface but here we focus on the residual structure in the abundances which we expect to reflect the internal stability of the clusters.

The results for collision fragmentation consist of a set of fragment abundances for each projectile cluster. Typically, the abundance decreases very rapidly with increasing number of lost atoms but, due to the high sensitivity of detection (single ion counting) and the large flux of projectiles, we could follow the fragment distribution over several orders of magnitude in count rate.

Also for the fragment distributions shown in Figs. 2 and 3 there are strong short-range structures superimposed on the general trend of a strong decrease, and the relative abundances of neighboring fragments appear to be nearly independent of the size of the original cluster. One particularly clear example is the relative abundance of Cu_8^- and Cu_7^- produced by fragmentation of cluster beams from Cu_9^- to Cu_{12}^-. This feature is observed for Al colliding with H_2 and Xe and for Cu colliding with H_2. For Cu clusters with 14 to 19 atoms, the fragmentation by Xe collisions shows some deviation from this pattern, and for Al clusters, the pattern appears slightly distorted in a way that can best be seen around mass 13. However, the overall pattern of the regularities suggests that the structure in the fragment spectra is specific to the clusters and not to the mechanisms of the collision process.

IV. DISCUSSION

The overall shape of the measured source abundances reflects the sputtering process in the source, the ion-optical selection in the acceleration stage, and the decay through electron emission of the presumably hot clusters at all points of their trajectories. Evaporation only affects the *local* structure of the spectrum since it just shifts the mass of the ions by one or two units. We expect the ion-optical selectivity to be of minor importance compared to the observed strong decrease of the current with increasing cluster size since, for example, nA currents of the heavy C_{60}^- anions are routinely delivered by the accelerator. Hence, the determining factor for the gross features of the spectra is the sputter process and, potentially, the subsequent electron emission from the cluster ions. Abundance spectra for metal clusters have been reported earlier and are usually fitted by a power law with powers $n=-5$ to -8 [2,6]. Fitting our data with a power law yielded powers of $n=-7.3$ (Al), $n=-6.0$ (Co), $n=-10$ (Ni), and $n=-5.2$ (Cu), in good agreement with the literature values for similar sputter energies. However, in our case, power-law fits do not reproduce the experimentally ob-

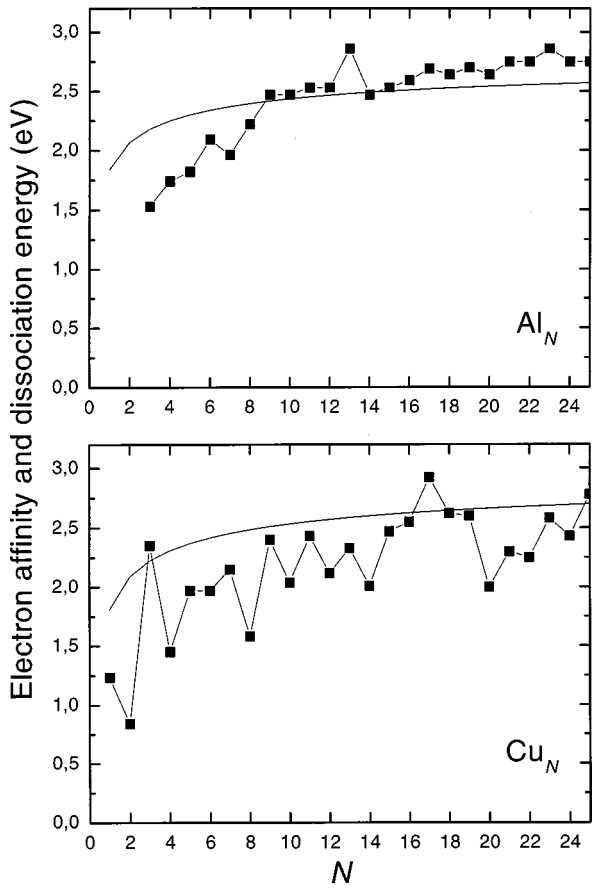

FIG. 6. Electron affinities for Al_N and Cu_N. The solid line is a liquid drop model calculation for single atom evaporation, based on the macroscopic evaporation enthalpies and surface tensions.

served smooth trends in the data very well. We note that although the power of $n=-6.0$ for Co is similar to those for Al and Cu, the overall intensity of Co (and Ni) anions produced by sputtering is, as mentioned previously, much smaller than for Al and Cu anions.

For fragmentation after gas collisions, the general trend is steeply decreasing fragment abundances with an increasing number of evaporations. Superposed on this general decrease one sees strong odd-even variations for both the Al and the Cu data. These variations seem almost independent of the target gas. Also the suppression of the odd-even effect in Cu above $N=10$ and the prominent shell closing in Al at $N=13$ appear independently of the target composition. For Al below $N=5$ and for Cu above $N=17$ the spectra deviate, mainly due to statistics.

The variations for Cu follow from $N=2$ to $N=10$ very closely the variations in the electron affinities [7,8], shown in Fig. 6. For N greater than 10, the fragment abundances appear to be less sensitive to variations in the electron affinity. Since the electron affinity is a measure of the stability of the clusters, the correlation between the neighboring abundances and the electron affinities is a further indication that the form of the spectra is determined by cluster stability. For monovalent clusters, evaporation of an atom reduces the number of valence electrons by one, and since the local variations with N of the cluster stability are dominated by the contribution from valence electrons, the stability against evaporation is strongly correlated with the electron affinity (see [9,10] for a comparison between electron affinities of silver clusters of size N and dissociation energies of silver cations of size $N+2$). The observed correlation between fragment abundances and electron affinities for the copper clusters therefore does not imply that the decay is dominated by electron emission but could be due to a correlation of the fragment abundancies with the stability against dissociation.

The dissociation energy D_N for clusters can be extrapolated from bulk values of cohesive energy and surface tension (see, e.g., [11]). The extrapolation is based on the liquid drop model,

$$D_N = A - BN^{-1/3}, \tag{1}$$

with parameters A and B determined from the bulk heat of evaporation and the surface tension, $A=2.95$ eV and $B=1.11$ eV for Al, and $A=3.16$ eV and $B=1.35$ eV for Cu. This extrapolation is shown as solid lines in Fig. 6 and indicates a dissociation energy similar to, or higher than, the electron affinity. Atoms are emitted more easily than electrons for identical activation energies as was noted in [12]. This is a consequence of the difference in phase space associated with the energy of the evaporating electron and the atom [13]. The ratio of the densities of states in the two cases is determined mainly by a factor m_a/m_e which for Cu amounts to a factor of 10^5 [see Eqs. (2) and (3) below]. Consequently, even for dissociation energies higher than the electron affinities the dominant process may still be atomic evaporation.

The magnet scan abundances of Cu clusters in Fig. 5 also exhibit a strong similarity with the fragmentation data in Fig. 3 and an even stronger similarity with the electron affinities. There is therefore little doubt that the abundances in the spectra of Cu_N^- clusters, generated either from collisions or from the source, are determined by the energetics of the clusters. The indication from the data is that the stability enters through the thermal emission processes. In the fragmentation experiment, collisions in the gas cell provide the internal energy necessary for evaporation and, similarly, clusters are created in the sputter source with high internal energy. Measurements of the decay of negative metal cluster beams produced with the same source and stored in the recently commissioned electrostatic ion storage ring ELISA confirm that a significant fraction of the clusters are produced with enough internal energy to undergo at least one fragmentation (or electron emission) on the submillisecond time scale [14].

The Al collision data also compare well with the electron affinities [15] although there is a serious discrepancy at $N=5-7$ where local maxima and minima of the electron affinity and the abundances are out of phase. We have as yet no explanation for this observation. In contrast, the $N=13$ (corresponding to 40 valence electrons) shell closing appears very prominently in the Al magnet scan, in the fragmentation data, and in the electron affinities. Overall, the magnet scan shows a better correlation with the electron affinities than do the collision data.

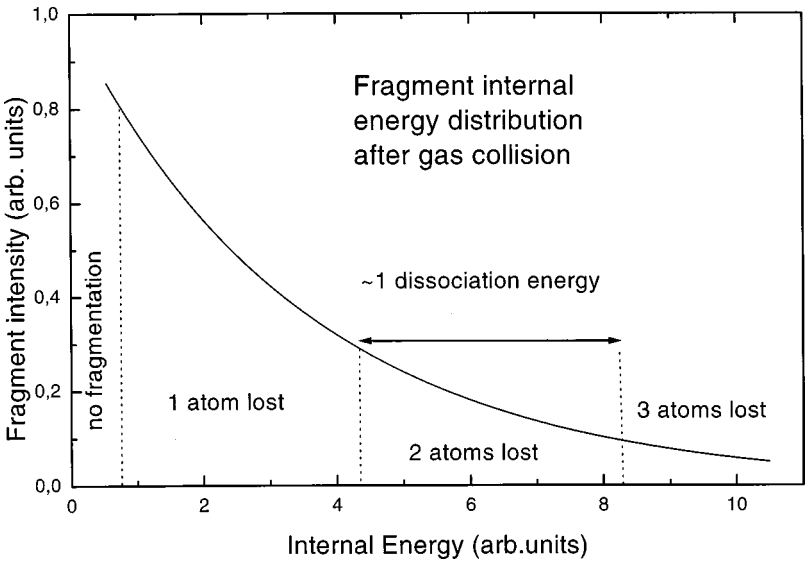

FIG. 7. Qualitative illustration of the energy distribution after collision. The vertical dotted lines divide roughly between regions corresponding to eventual loss of 0, 1, 2, or 3 atoms.

As argued above, the presence of the characteristic odd-even alternations in the spectra and the locally enhanced intensities at the shell closings strongly suggest that these spectra are formed through mechanisms where the last step is an evaporative process of the unimolecular type at relatively low internal energy. This suggestion is corroborated by the fact that the average number of atoms lost after collisions is relatively small. A small relative loss either indicates a prompt and possibly very energetic ejection of a small fragment or a slow low-energy process of unimolecular type. Since only the latter can be expected to reflect the internal stability of the cluster this is the most likely scenario. It is, on the other hand, not possible to exclude more direct knock-out processes. It is well known that for clusters of the small sizes relevant here, the cluster stabilities determine abundance variations unambiguously if only the last decay process is of the delayed, low-energy type.

Similar considerations apply to the source abundance spectra. In particular, it is not possible to say what initial cluster sizes give rise to a given observed size, only that most clusters have undergone at least one decay after commencing free flight above the cathode surface.

We now discuss the shape of the smooth trend of the fragmentation spectra. When only sequential evaporation is involved in the decays, the number of evaporated atoms is limited by the available energy. In this case, the spectra therefore reflect the energy distribution imparted in the collision. This is illustrated qualitatively in Fig. 7 where the curve represents the distribution in cluster internal energy immediately after the collision. Since decay rates depend strongly on degree of excitation there will be a fairly sharp energy threshold for loss of one additional atom from the cluster during the time of flight from the collision cell to the mass analyzer. This means that a given internal energy leads to the loss of a definite number of atoms and the observed fragment abundance is proportional to the integrated distribution between two consecutive thresholds. With this interpretation the steep, nearly exponential population curves observed for many of the clusters (Figs. 2 and 3) would correspond to a steeply decreasing, nearly exponential distribution in excitation energy.

To estimate the shape of the distribution in excitation energy after passage of the gas cell, we have approximated the cross section by a sum of screened Coulomb cross sections for atom-atom collisions. For both Al and Cu clusters colliding with hydrogen atoms at the c.m. energies in the present experiment the impact parameter is well below 1 Å for atom-atom collisions leading to significant excitation, and the ansatz therefore seems justified as a first approximation. The resulting distribution in collisional excitation energy E is, however, far from being exponential. The distribution is much flatter, scaling approximately as $E^{-3/2}$.

A plausible explanation for the discrepancy is the competition by electron emission since the electron affinity and the atomic binding are of the same order for the clusters studied. If the branching ratio between electron loss and emission of an atom is nearly the same in consecutive evaporations, this competition may indeed lead to nearly exponential fragment distributions [16]. Supporting evidence for this explanation was obtained from a comparison of total destruction cross sections with the total yield of negative fragments which indicated that a substantial fraction of the excited clusters were neutralized and hence not detected.

V. SIMULATIONS

In order to evaluate quantitatively the influence of electron emission on the fragment distributions, a Monte Carlo simulation of the postcollisional fragmentation pattern was performed. The rates were assumed to be given in terms of the level densities ρ as in [13],

$$k(E)=\frac{2m_a}{\pi^2\hbar^3}\sigma_{geo}\ (k_BT_d)^2\ \frac{\rho_{daughter}(E-D)}{\rho_{parent}(E)} \qquad (2)$$

for the atomic evaporation, and

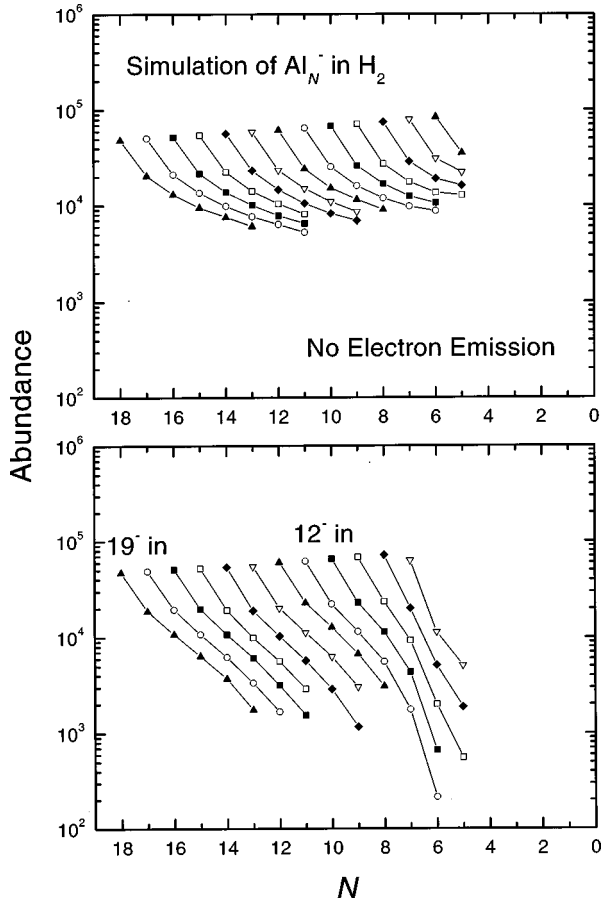

FIG. 8. Simulations of the fragment size distribution after passage of an aluminum cluster through a cell with H_2 gas. The lines connect fragments from the same parent cluster, the highest N corresponding to loss of a single atom. The upper graph shows the results from a simulation without electron emission but with otherwise identical conditions.

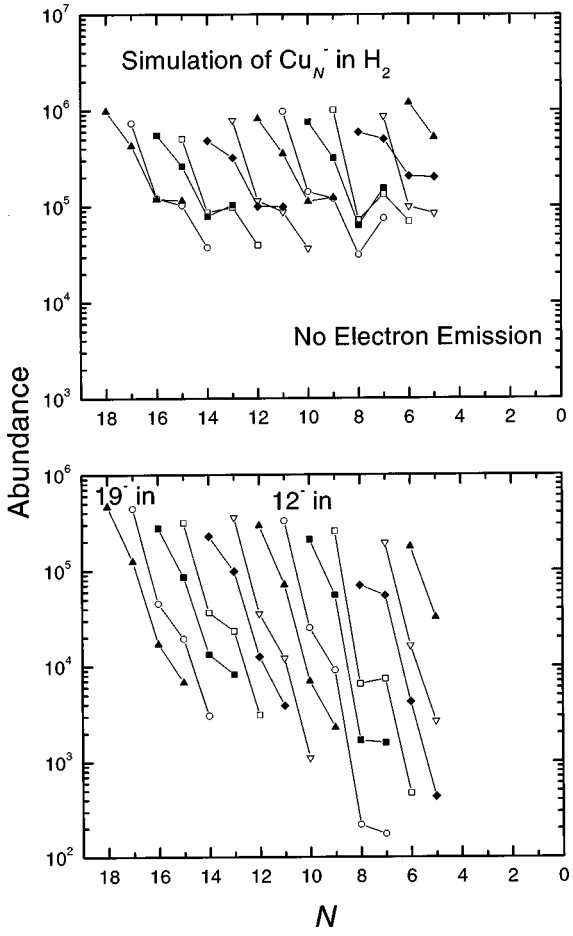

FIG. 9. As Fig. 8 but for Cu clusters.

$$k(E)=\frac{2m_e}{\pi^2\hbar^3}\sigma_{pol}\ (k_BT_d)^2\ \frac{\rho_{daughter}(E-E_A)}{\rho_{parent}(E)} \qquad (3)$$

for the electron emission. Here m_a is the mass of the atom lost, m_e the mass of the electron, D the atomic dissociation energy, E_A the electron affinity, T_d the microcanonical temperature of the daughter cluster, k_B Boltzmann's constant, and σ_{geo} the geometrical cross section of the cluster. With an absorption-on-contact electron-capture cross section proportional to the electron kinetic energy to the power $-1/2$, the value of the Langevin cross section averaged over the energy distribution is $\sigma_{pol}=\pi\sqrt{\alpha\pi e^2/(2k_BT_d)}$, where α is the static polarizability of the cluster, taken to be Nr_s^3 (ESU) with r_s the Wigner-Seitz radius, and e is the electron charge. As the atomic binding energies are unknown the liquid drop value in Eq. (1) was used as a first estimate for both Al and Cu. For the Cu clusters, the shell energy and odd-even effects in the measured electron affinity were obtained by the subtraction of a smooth function from the data in Fig. 6 and then added to the liquid drop curve in the same figure to obtain a more realistic estimate of the local variation with size of the dissociation energy. Such a procedure is well known in nuclear physics and has also been applied to metal clusters in connection with shell structure calculations [11]. The procedure could not be applied for Al clusters since Al is trivalent and consequently the deviations from the liquid drop value of the dissociation energy cannot be correlated with similar quantities for the electron binding. For the atomic binding in Al clusters we therefore used the liquid drop value. For neither the Al nor the Cu clusters was dimer evaporation taken into account.

The level density function in the rate constants was approximated by the high–temperature limit of the level density of a collection of quantum-mechanical harmonic oscillators with frequencies ν_i, i.e., $\rho(E)\propto(E+E_0)^{3N-7}$, with $E_0=\Sigma_i h\nu_i/2$ being the zero point energy of the oscillators. For the constant of proportionality we used the Kassel value, $1/(3N-7)!\Pi_i h\nu_i$ [17] and all frequencies were set equal to the Debye frequency of the bulk material.

The simulations followed one specific cluster ion from its formation in the source with an internal energy distributed exponentially with characteristic energy $(3N-6)/10$ eV through mass selection, the flight through the magnet, and the subsequent flight to the collision cell. Loss of an electron before or during passage through the magnet rendered the cluster unobservable; electron loss after the magnet and be-

fore detection was counted as loss due to neutralization. The cluster anions that reached the collision cell were given an energy according to the distribution $\rho_{exc} \propto (E+E_c)^{-p}$, with $p=1.36$ and $E_c=0.05$ eV for Al, and $p=1.55$ and $E_c=0.177$ eV for Cu. These distributions were obtained from fits to screened Coulomb cross sections for binary collisions of Al or Cu atoms with hydrogen atoms, as mentioned above. After collision, the fragmentation of the excited clusters proceeded in a manner similar to the precollision decay, i.e., until either the charge was lost by electron emission or the time for decay was so long that the cluster was detected before decaying. Each postcollisional fragment was recorded with resulting size and parent size, exactly as in the experiments. A total of 2×10^8 clusters were followed from the source for both Al and Cu clusters. The decay chains were terminated when the cluster reached $N=4$ in order to be able to represent the daughter clusters with the level density given above.

The simulated spectra are shown in Figs. 8 and 9. For comparison, the spectra with no electron emission but otherwise identical conditions are also shown. The importance of electron emission in providing a nearly exponential cutoff of the fragment abundances is obvious. The logarithmic slope is quite sensitive to the magnitude of the electron emission rate in Eq. (3), which has been divided by factors 10 and 5 for Al and Cu clusters, respectively, to obtain better accord with the measurement. The reduction factors may be interpreted as sticking coefficients of order 0.1 in the reverse process of electron attachment, and similar or larger reductions are typically reported in the literature [18]. The spectra generated without taking electron emission into account, on the other hand, are similar to the collisional energy transfer distribution as expected. For Al the slope of the fragment distributions changes with cluster size, and this feature is reproduced by the simulation. The reason is the fairly strong variation with N of the relative magnitude of the electron affinity and the dissociation energy. However, the detailed agreement is better for Cu where the local variation of the dissociation energy could be estimated. The conclusion is that the essential features of the fragmentation spectra can be reproduced by the model and this supports the explanation in terms of a competition between statistical evaporation of atoms and electrons from excited clusters.

VI. CONCLUSION

We have measured the variation with cluster size of the beam intensity for Al_N and Cu_N anions produced in a sputter source. We have also measured abundance spectra for fragmentation of individual beams of Al_N and Cu_N anions with cluster sizes between $N=4$ and $N=19$ and the local variations have been compared with the analogous variations in the source yields.

The source and fragmentation distributions show a strong similarity in the local variations which are also correlated with the measured electron affinities for Al_N and Cu_N. We conclude that this similarity is caused by postproduction and postcollisional thermal fragmentation of the clusters and/or thermal electron emission. Hence most clusters are produced in the source with sufficient energy that one or more thermal decay processes occur before mass selection. Similarly, the collision products contain enough energy to fragment or emit an electron before reaching the analyzer. On the other hand, the energy content is low enough to ensure that the relative mass loss is small and that the decay is determined by the internal stability of the cluster, i.e. that the decay is an activated process.

We have obtained strong evidence for electron emission being an important competing channel for decay of hot, negatively charged Al and Cu clusters, both from a comparison of negative-fragment yields with the loss of parent clusters and from a simulation of the size distribution of negative fragments after gas collisions. Neutralization by electron emission offers a simple explanation of the nearly exponential decrease of the yield with the number of evaporated atoms, which is observed for Cu and for the smaller Al clusters. For the local structure in the distributions this competition is not so important because of the strong correlation between the atomic binding and the electron affinity, especially for the monovalent Cu.

ACKNOWLEDGMENTS

This work has been supported by the Danish National Research Foundation through the Aarhus Center for Atomic Physics (ACAP) and by NATO Grant No. 960122.

[1] W. D. Knight, K. Clemenger, W. A. de Heer, W. A. Saunders, M. Y. Chou, and M. L. Cohen, Phys. Rev. Lett. **52**, 2141 (1984).
[2] I. Katakuse, T. Ichihara, Y. Fujita, T. Matsuo, T. Sakurai, and H. Matsuda, Int. J. Mass Spectrom. Ion Processes **67**, 229 (1985).
[3] W. A. de Heer, Rev. Mod. Phys. **65**, 611 (1993).
[4] P. T. Kesson, P. Tykesson, H. H. Andersen, and J. Heinemeier, IEEE Trans. Nucl. Sci. **23**, 1104 (1976).
[5] H. Shen, P. Hvelplund, D. Mathur, A. Bárány, H. Cederquist, N. Selberg, and D. C. Lorents, Phys. Rev. A **52**, 3847 (1995).
[6] A. Wucher and M. Wahl, Nucl. Instrum. Methods Phys. Res. B **115**, 581 (1996).
[7] D. G. Leopold, J. Ho, and W. C. Lineberger, J. Chem. Phys. **86**, 1715 (1987).
[8] C. L. Pettiette, S. H. Yang, M. J. Craycraft, J. Conceicao, R. T. Laaksonen, O. Cheshnovsky, and R. E. Smalley, J. Chem. Phys. **88**, 5377 (1988).
[9] J. Ho, K. M. Ervin, and W. C. Lineberger, J. Chem. Phys. **93**, 6987 (1990).
[10] S. Krückeberg, G. Dietrich, K. Lützenkirchen, L. Sweikhard, C. Walther, and J. Ziegler, J. Chem. Phys. **110**, 7216 (1999).
[11] H. Nishioka, K. Hansen, and B. R. Mottelson, Phys. Rev. B **42**, 9377 (1990).
[12] G. Ganteför, W. Eberhardt, H. Weidele, D. Kreisle, and E.

Recknagel, Phys. Rev. Lett. **77**, 4524 (1996).
[13] K. Hansen, Philos. Mag. B **79**, 510 (1999).
[14] K. Hansen *et al.* (unpublished).
[15] K. J. Taylor, C. L. Pettiette, M. J. Craycraft, O. Chesnovsky, and R. E. Smalley, Chem. Phys. Lett. **152**, 347 (1988).
[16] P. Hvelplund, L. H. Andersen, H. K. Haugen, J. Lindhard, D. C. Lorents, R. Malhotra, and R. Ruoff, Phys. Rev. Lett. **69**, 1915 (1992).
[17] M. R. Hoare and Th. W. Ruijgrok, J. Chem. Phys. **52**, 113 (1970).
[18] A. H. Amrein, R. Simpson, and P. Hackett, J. Chem. Phys. **95**, 1781 (1991).